ELECTRIC VEHICLES CHARGING

Management and Control Strategies

Filipe J. Soares, David Rua, Clara Gouveia, Bruna D. Tavares, António M. Coelho, and João A.P. Lopes

xxxxxx

In this article, we present a holistic framework for the integration of electric vehicles (EVs) in electric power systems. Their charging management and control methodologies must be optimized to minimize the negative impact of the charging process on the grid and maximize the benefits that charging controllability may bring to their owners, energy retailers, and system operators. We have assessed the performance of these methods initially through steady-state computational simulations, and then we validated them in a microgrid (MG) laboratory environment.

Climate Change

Global warming is one of the environmental reasons for leveraging the large-scale adoption of EVs. According to the Organisation for Economic Cooperation and Development, the transportation sector accounts for more than 50% of the world's oil consumption and is responsible for approximately 20% of the world's carbon-dioxide emissions. Therefore, the transportation sector is naturally one of the principal targets of countries' policies to mitigate climate change.

Digital Object Identifier 10.1109/MVT.2017.2781538
Date of publication: 29 January 2018

Power System Impacts

While the integration of moderate quantities of EVs into the electric power system does not provoke any considerable impact, their broad adoption will likely create technical problems with regard to grid operation and management [1]–[3]. To overcome these issues, two paths can be followed: reinforce the existing infrastructures and plan new networks so that they can handle the EV integration, or develop and implement enhanced charging-management strategies capable of controlling EV charging according to the capabilities of a given grid. While the former is an expensive solution that will require significant investment in network infrastructures, the latter yields other

benefits from the grid perspective because it provides elasticity to the EV loads [4]–[7].

Given this context, and considering the expected growth in EV integration, detailed studies about the impact of integrating EVs in power systems should be performed to evaluate the best approaches to follow in the future. These studies will require the development of comprehensive and standardized EV models and simulation tools that can be used in a wide variety of scenarios, including different EV types and power systems with distinct characteristics [8].

EV-Integration Architecture

The technical management of an electric power system undergoing a large-scale deployment of EVs will require the combination of a centralized hierarchical management and a control structure with a local control located at the EV grid interface based on the MG concept to accommodate EV battery charging [9], [10]. The simple use of a smart device interfacing the EV with the grid does not solve all of the problems raised by EV integration in distribution networks. These interfaces can be effective when dealing with the occurrence of voltage drops that may be caused by EV charging, locally decreasing the charging rate through a voltage droop control approach. However, this local solution fails to address issues that require a higher control level, such as managing branch congestion levels or enabling EVs to participate in the electricity markets. For these cases, coordinated control is required, and a hierarchical management and control structure that is responsible for the entire grid operation, including EV management, must be available. Therefore, the efficient operation of such a system depends on the combination and coordination of local and centralized control modes. The latter control approach also relies on the creation of an adequate communications infrastructure [11] capable of handling all the information that needs to be exchanged between EV and the central control entities organized in a hierarchical structure.

Normal System Operation

When operating the grid under normal conditions, EVs will be managed and controlled by a new (central) entity, the aggregator, whose main functionality will be to group EVs, according to the willingness of their owners, to exploit business opportunities in the electricity markets [12]. If EVs were to enter the electricity markets on an individual basis, then their visibility would be slight and unreliable due to their stochastic behavior. However, if an aggregating entity were to exist that could group EVs and enter them into market negotiations, then the provided services would be more significant and the confidence in its availability prediction would be much more accurate. The aggregator should always take into account the preferences of the owners, so that it can provide them with information about power demands and connection periods via, e.g., smart meters. In the same regional area, several aggregators might coexist and compete to gather as many clients as possible. This competition will be beneficial for the EV owners, who will be able to choose as their aggregator the company that best fits their needs. Given the complexity of the information that an aggregator needs to collect and process, a hierarchical management structure, independent from the distribution system operator (DSO), is suggested in this article (Figure 1).

Because each aggregator develops its activities across a large geographical area, e.g., a country, it will comprise two different types of entities: the regional aggregation unit (RAU) and the MGAU. The RAU is considered to be at the high-voltage (HV)/medium-voltage (MV) substation level, with possibly 20,000 customers, communicating with several downstream MGAUs, which, in turn, will be at the MV/low-voltage (LV) substation level, with roughly 400 customers each. The RAU and the MGAU were created to decrease communications and the computational burden that would be required in a real implementation of this concept. This will provide the aggregator with preprocessed information regarding groups of EVs located in the LV and MV grids. Each EV must have a specific interface unit, the vehicle controller (VC), to enable bidirectional communications between the EV and the upstream aggregator. The VC will be located in each EV's smart meter, and the smart-meter communication infrastructure should be used to support this architecture. In addition to the VC, there is a new type of element, the cluster of vehicles controller (CVC), which is designed to control energy charging for large parking lots (e.g., shopping centers) and is fed directly from the MV network. Individual EV controllers under CVC management do not need an active VC communicating with upstream hierarchical controllers. For normal operations, the VC will interact with the MGAU, while the CVC will interact directly with the RAU.

Abnormal System Operation or Emergency Mode

When the technical operation of the grid is compromised, the market management can be overridden by the DSO through the technical operation control hierarchy, as shown in Figure 2. For these abnormal or emergency conditions, it makes sense to adopt the MG and multi-MG (MMG) [13] concepts. In fact, the MG and MMG already account for the existence of a hierarchical monitoring and management solution, including a suitable communications infrastructure, that is capable of managing the presence of EVs connected either individually at the LV level or as a cluster (e.g., a fleet charging station or a fast-charging station) at the MV level. Within a LV MG, a MG central controller (MGCC) may control EV batteries through the VC. As depicted in Figure 2, within a MMG environment, the elements of the MV grid, including the MG and CVC, can be technically managed by the central autonomous management controller

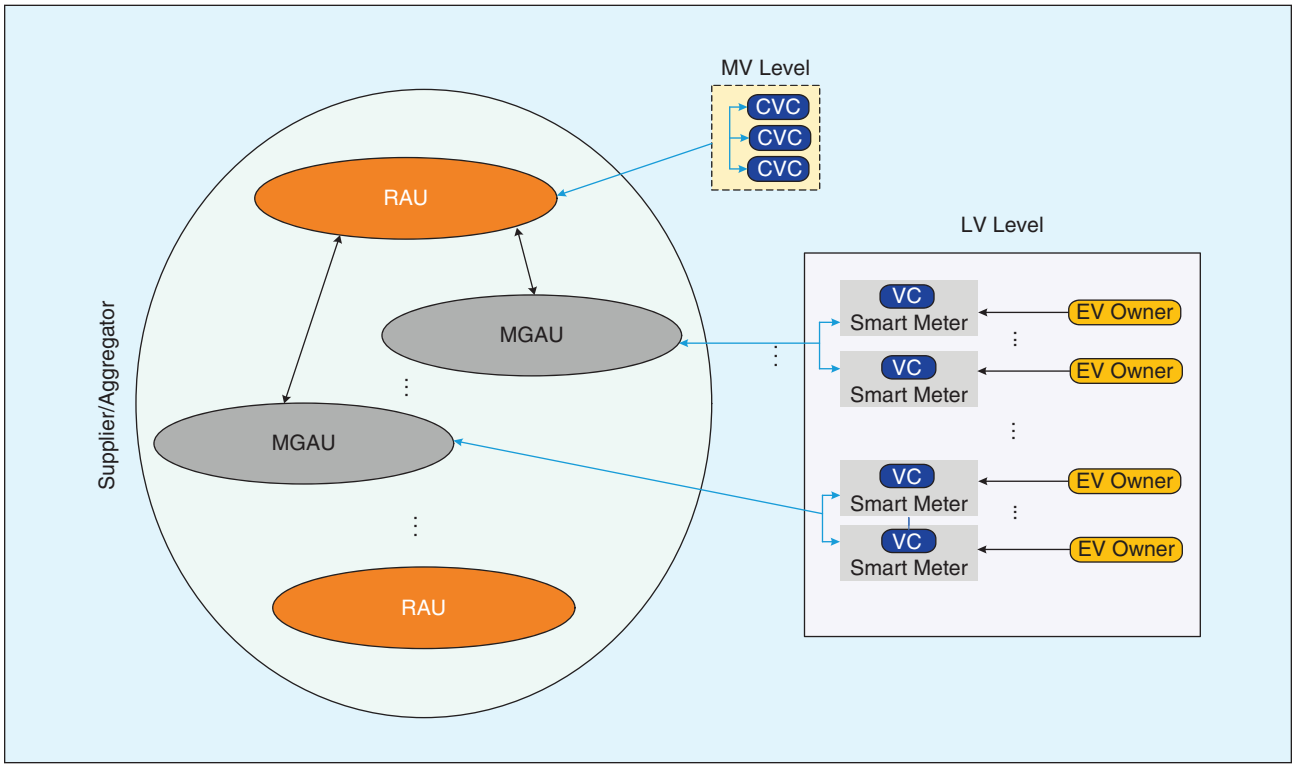

FIGURE 1 The aggregators' hierarchical management structure.

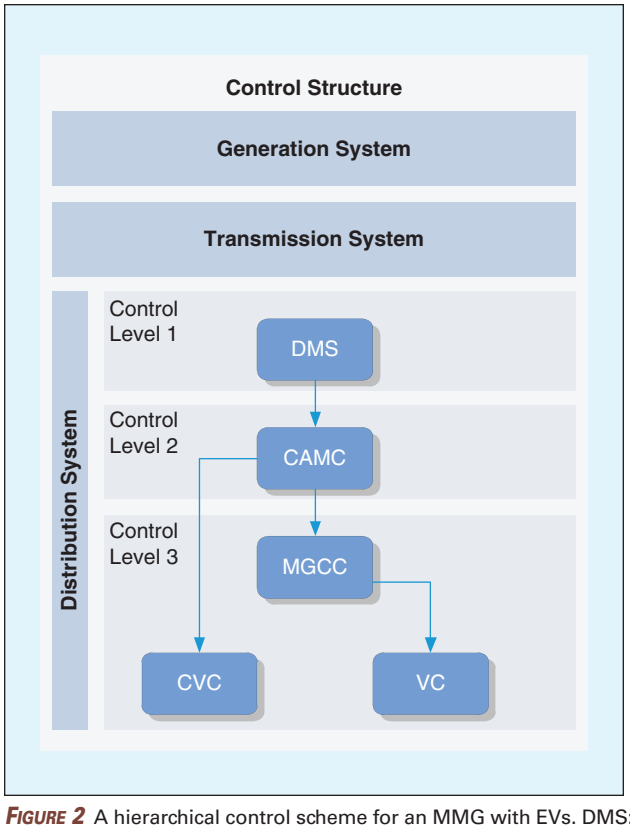

FIGURE 2 A hierarchical control scheme for an MMG with EVs. DMS: distribution management system; CAMC: central autonomous management controller.

(CAMC), a control entity to be installed in the HV/MV substation. All CAMCs will be under the supervision of a single distribution management system (DMS), which is directly controlled by the DSO. In abnormal system operation conditions or in emergency modes, all technical management and control tasks are the responsibility of the DSO and are performed by a main control entity, the DMS, and by the other distributed entities, the CAMC and the MGCC.

Steady-State Simulations

The large deployment of EVs is very likely to provoke changes in power-demand patterns, causing alterations in the grids' voltage profiles, branches' congestion levels, and energy losses, i.e., at the distribution level where the EVs will connect. Thus, it is important for the DSO to develop new approaches to evaluate their impact in distribution networks. The approach we present in this article assumes that the load inherent to EV charging will appear in the grid nodes proportionally to the residential power installed in each node. This approach also allows the evaluation of the maximum number of EVs that can be safely integrated in a given network when three charging strategies are implemented: dumb charging, multiple tariff, and smart charging [12].

The proposed methodology is essentially focused on determining the locations and time periods during which EVs will plug in to charge when the three charging

strategies are adopted. The EV battery charging was assumed to be performed at a constant power rate of 3 kW. We also considered that the EV batteries' state of charge at the moment it is plugged in is unknown. For this reason, an average charging time of 4 h was assumed for all of the EVs. Assuming an energy consumption of 0.2 kWh/km, the daily energy absorbed (12 kWh) would be enough for traveling approximately 60 km without needing to recharge.

The first step of the methodology is to define the time period during which each EV will be connected to the grid. For that, it is assumed that EVs only make two journeys per day and that they are plugged in only in the time periods between the last journey of one day and the first journey of the next day. The two moments when EVs make their daily journeys are asserted using the probability distribution presented in Figure 3, with a consistent minimum connection time of 4 h. The second step of the approach is to define the periods during which EVs will effectively charge. These periods will vary in accordance with the charging strategy under consideration, as mentioned in [9].

In this approach, smart charging is formulated as an optimization problem that has the objective of minimizing the networks' peak load:

$$\min\left[\max_{t=1:24h}\left(\sum_{j=1}^{m} CL_t^j + \sum_{i=1}^{n}(EVC_t^i)\times 3\right)\right], \tag{1}$$

subject to:

$$\sum_{t=1}^{24} EVC_t^i = 4, \begin{cases} i\in[1,n] \\ t\in[1,24] \end{cases} \tag{2}$$

and

$$EVP_t^i \geq EVC_t^i, \begin{cases} k\in[1,n] \\ t\in[1,24] \end{cases}, \tag{3}$$

where $\max(CL_t^j + \Sigma_{i=1}^{n}(EVC_t^i)\times 3)$ is the peak power (kW); CL_t^j is the conventional load in the bus j (kW) in the time step t; EVC_t^i includes the periods t when EV_i will charge, i.e., if $EVC_t^i = 1$, then EV_i will charge in moment t, but if $EVC_t^i = 0$, then EV_i will not charge. The $n\times 24$ binary variables EVC_t^i are the decision variables of the optimization problem; t is the time step index; i is the EV index; n is the total number of EVs in the grid area; j is the bus index; m is the number of buses in the network; and EVP_t^i is used to define the periods t when EV_i is parked and plugged in to the grid.

The equality constraint presented in (2) assures that all EVs will charge for exactly 4 h, whereas the condition implemented in (3) assures that EVs will only charge when they are plugged in. The constant 3 presented in (1) is the charging rate, in kilowatts, and is assumed for all EVs. After determining the periods when EVs will charge, the network buses where EVs will plug in for charging are calculated, taking into account the proportion of residential

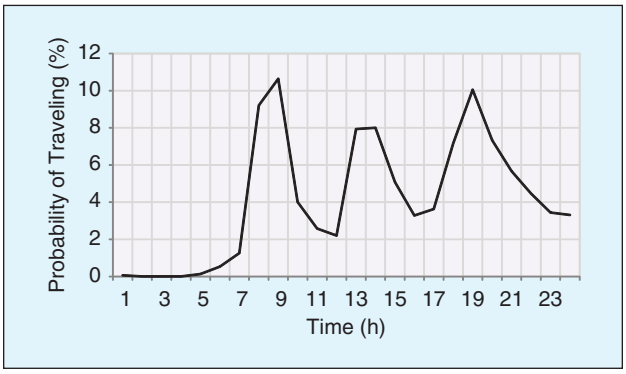

FIGURE 3 The probability distribution used to define the EV daily journeys [14].

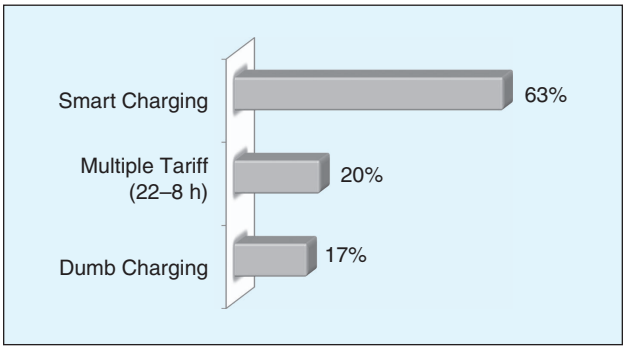

FIGURE 4 The allowable EV integration in an MV grid from a semiurban area.

power installed in each node. Then, all EVs are tagged with a bus number, indicating the bus where they plug in for charging. Finally, the total load in the grid is calculated by adding the conventional load to the respective EV load.

The impact of EVs on an MV grid from a semiurban area, used as a test case, is evaluated using the described methodology. First, the number of EVs that can be safely integrated into the grid is evaluated while considering all EVs as dumb charging, multiple tariff, and smart charging adherents. Then, three more simulations are performed to evaluate the effectiveness of the smart charging when compared with the dumb charging and with the multiple tariff, regarding the impacts in the grid operating conditions. The maximum allowable EV integration in the grid is presented in Figure 4. The percentages are relative to the total number of conventional vehicles in the geographical area covered by this network, which is approximately 12,700 EVs. Figure 5 shows the changes in the load diagrams for the different charging strategies, with an EV integration of 63%. The worst bus voltage is presented in Figure 6.

Figure 7 shows an overview of the lines loading for the scenarios studied, further illustrating the impact of the three charging strategies in this matter. Figure 8 shows the absolute values of losses for the selected day (bars) on the left axis and their value, relative to the overall energy consumption (squares), on the right axis. As

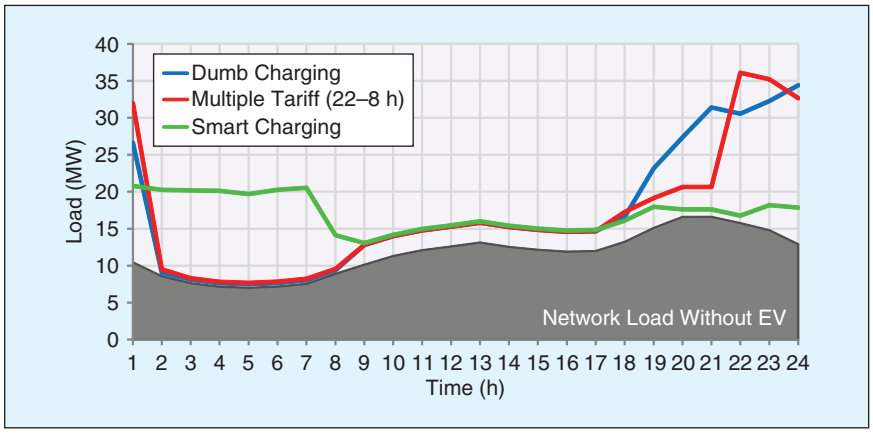

Figure 5 Changes in the load diagram with an EV integration of 63%.

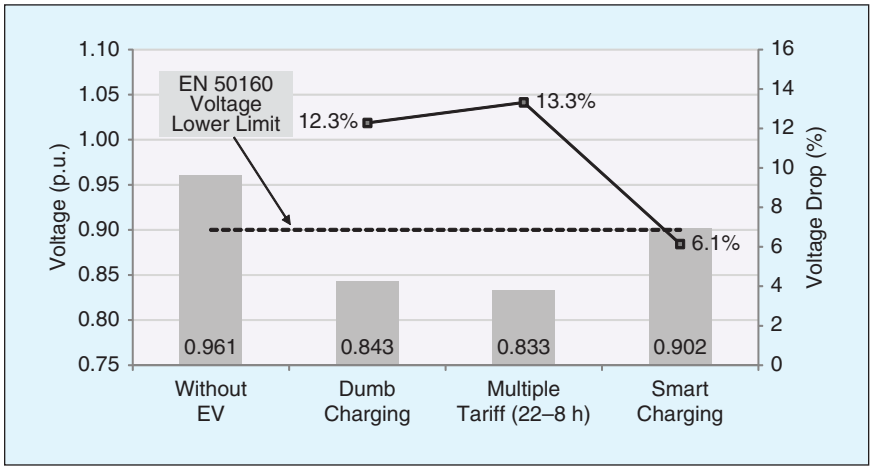

Figure 6 The worst bus voltage, with an EN 50160 [15] voltage lower limit. p.u.: per unit.

expected, smart charging achieves the best result because it optimizes the load distribution during the day, minimizing the occurrence of high peak loads when the consumption reaches very high values. The peak load periods are the most critical for the losses as they are proportional to the square of the current, which is very high in such conditions.

Experimental Validation of EV Management and Control Methods

Infrastructure

The laboratory wherein we tested the performance of the developed control and management concepts was created to be a flexible and scalable structure to allow the individual and integrated testing of new concepts and control algorithms, which would be housed at different hierarchical levels of the smart grids, as well as different communication architectures, technologies, and protocols. The laboratory's electric and automation equipment included renewable energy-based microgeneration (3-kW wind microturbine emulator and 6-kWp photovoltaic panels), storage (with 25-kWh capacity flooded lead-acid battery banks and 128 lithium-ion battery cells for the EV charging prototype), a 54-kW resistive load bank, and a plug-in EV, which was charged by a single-phase commercial home charger. To implement the smart-charging and vehicle-to-grid strategies, a bidirectional inverter prototype was also available, connected to the lithium-ion battery cells. A group of SMA Sunny Island inverters were available to explore scenarios where the laboratory infrastructure was isolated from the electric grid.

A communications infrastructure was implemented as an overlay to the existing supervisory control and data acquisition (SCADA) system, allowing the implementation of a MG management and control structure. As shown in Figure 9, the management and control structure was implemented considering three levels: the distribution management and control system, which coordinated the operation of the distribution network; the MGCC, which ensured the management and control of the MG; and the lower control level, which was constituted by smart meters and associated with MG local controllers [i.e., a microsource controller (MC), load controller (LC), and VC]. The smart meter acted as a gateway between the MGCC and the local controllers, providing bidirectional communication capabilities. It was able to receive set-points from the MGCC and forward them downstream to local controllers, and it sent metering data and other types of information upstream. The smart meter also had local management and processing capability to integrate the owner's preferences regarding the participation in grid-support services and remote management of the load and generation.

The MG's high-level management and control functionalities were housed in the MGCC. The data received from the smart meters (e.g., the power generation, load, number of EVs, responsive loads, and power-quality indicators) were processed and aggregated according to the system operator needs. The received data were then used by local software modules that were responsible for managing

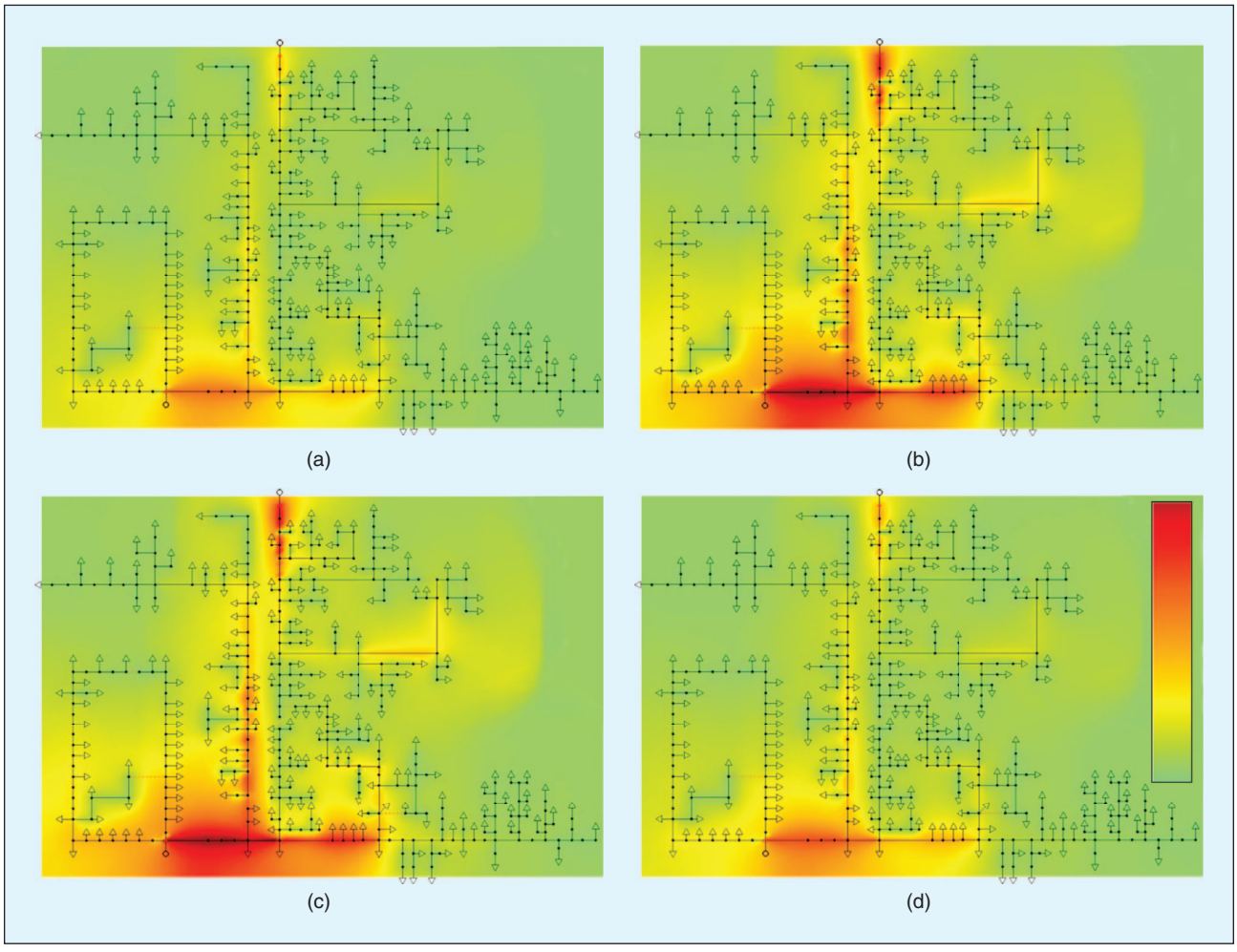

FIGURE 7 The line loading during the peak hour (a) without an EV, (b) dumb charging, (c) multiple tariff, and (d) smart charging.

the MG technical operation during normal and emergency conditions. An Ethernet infrastructure was used to interconnect the different elements of the control structure, thus providing a communication network between the different control levels and a means of interacting with the SCADA system. The network was also responsible for conveying the metered data from inverters, developed prototypes, and other laboratory equipment through the use of specific protocol converters. A medium-behavior controller was developed to allow the emulation of different communication technologies over the Ethernet infrastructure. A controllable communication medium was thus available where distributed medium-behavior controllers were able to impose controlled and variable bandwidth values and define different profiles of delays and data packet losses.

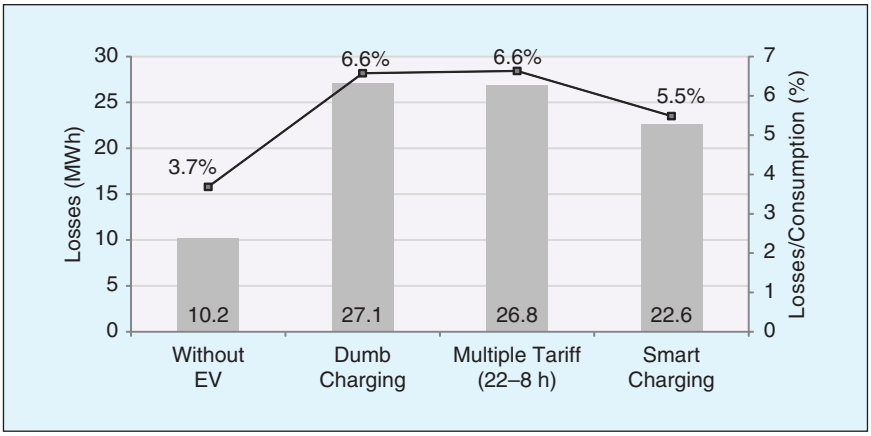

FIGURE 8 Energy losses in all of the studied scenarios (throughout the entire day).

Laboratory Tests

Interconnected Mode

The main objective of the MG test in the interconnected mode was to evaluate the performance of the power-voltage (P-V) droop control incorporated at the

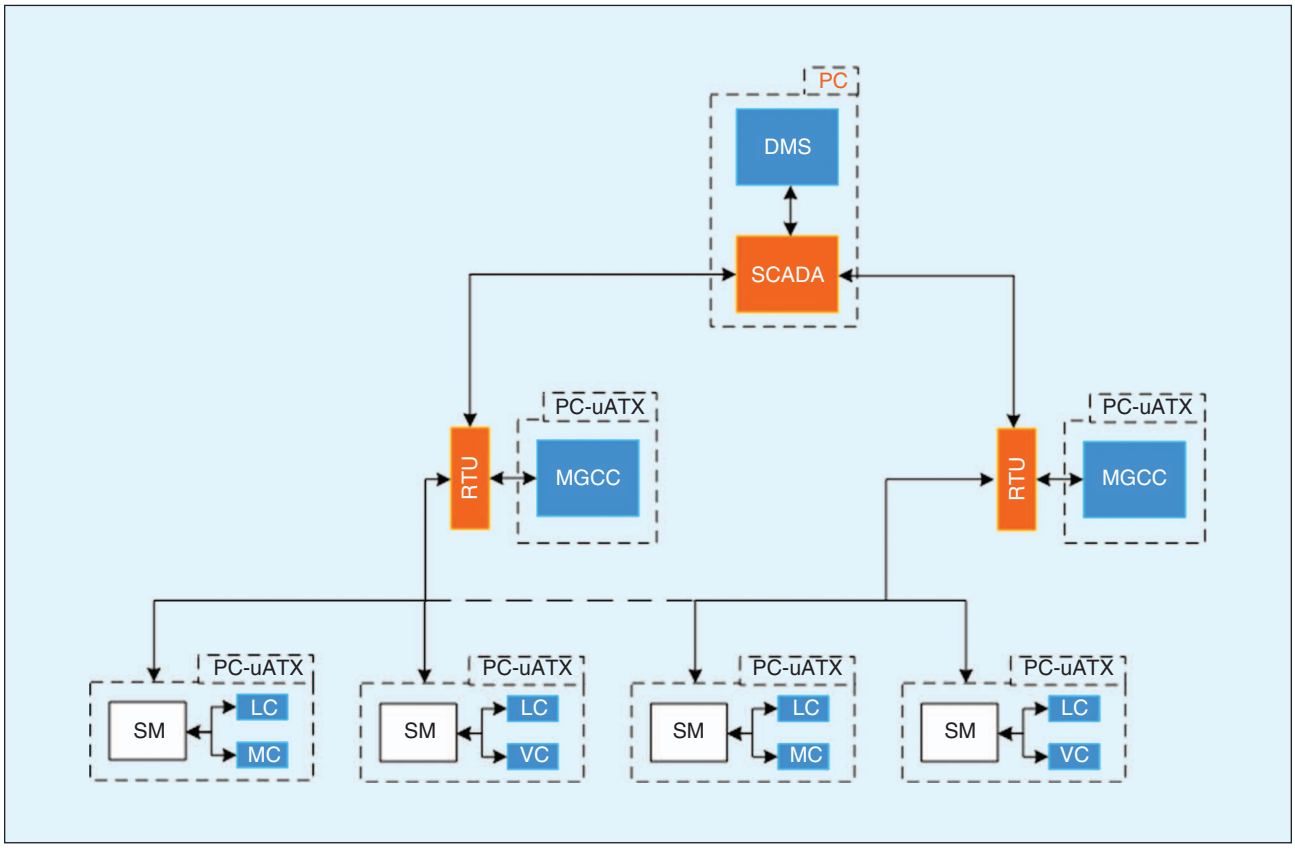

FIGURE 9 The laboratory management and control architecture. SM: smart meter; LC: load controller; MC: microsource controller; PC: personal computer; RTU: remote terminal unit; PC-uATX: personal computer micro-advanced technology extended motherboard.

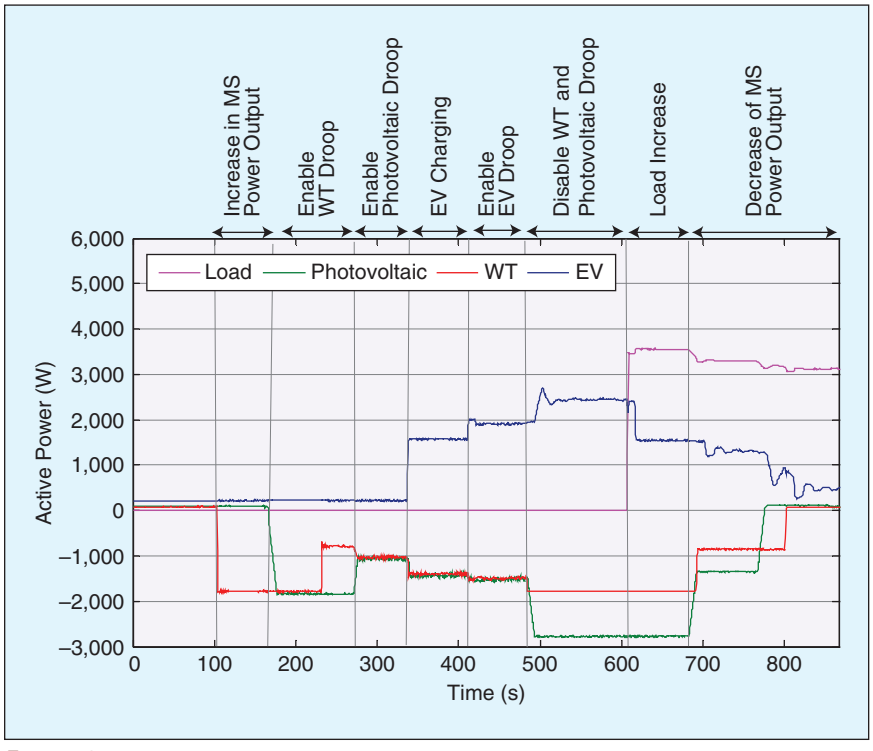

FIGURE 10 The main results of the MG interconnected scenario for test 1. MS: microsource; WT: wind turbine.

microgeneration units and at the EV power-electronic converters (i.e., single-phase units) and its remote parameterization through the MGCC. The simulated daily scenario considered a high penetration of renewable energy-based generation in low-load conditions. Figure 10 provides an overview of the results obtained. At $t = 104$ s, the microwind generator power production increased to approximately 1.8 kW. As shown in Figure 11, the voltage in phase A of node 2 suffered a significant increase. At $t = 167$ s, the photovoltaic panel began to inject power into the grid, causing a voltage increase from 240 to 247.2 V. As a result of the voltage value, the MGCC remotely sent a command to the EV to enable the droop control functionality in the microwind inverter at $t = 230$ s, reducing the active power injected by this unit and, subsequently, the phase

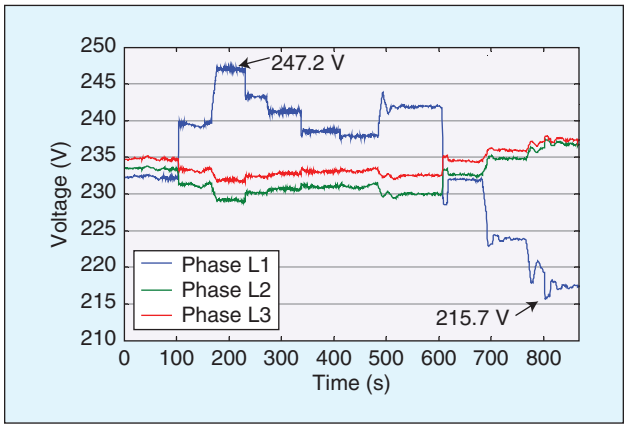

FIGURE 11 The voltage at node 2 for the MG interconnected scenario for test 1.

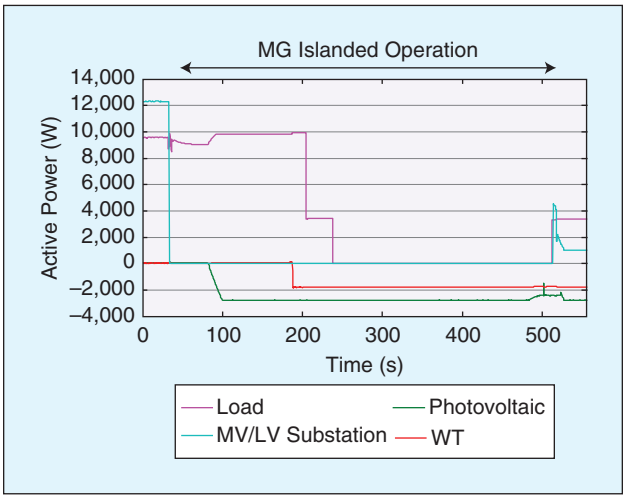

FIGURE 12 The main results of the MG islanded scenario.

voltage. At $t = 270$ s, the droop control functionality in the photovoltaic panel inverter was also activated. Both units had the same droop parameters, so they began to inject the same amount of active power and, thus, equally shared the power reduction.

At $t = 330$ s, the EV charger prototype was connected to the MG and began charging with a reference power of 1.5 kW. Because the MG load increased and the voltage decreased, the microgeneration units increased their power output. To show the effectiveness of the MG control strategy, the EV P-V droop was activated at $t = 410$ s, and the microgeneration units' voltage droop was disabled at $t = 480$ s. As shown in Figures 10 and 11, the microgeneration power output increased, thereby raising the MG voltage. As a consequence, the EV increased its power consumption to approximately 2.5 kW while maintaining the voltage at 242 V. At $t = 600$ s, a 3-kW load was connected, and the voltage dropped below 235 V. Because the voltage was within the EV droop dead band, the EV decreased the charging power to the reference value (1.5 kW). At $t = 680$ s, the power output from the microgeneration units started to decrease, simulating the end of the day. As a consequence, the voltage dropped below 225 V, surpassing the voltage dead band of the EV voltage droop control and resulting in the reduction of its charging power.

Islanded Mode

At the beginning of the experiment, the MG was connected to the main grid, importing approximately 12 kW from the upstream network. The EV prototype charged, and the microgeneration units remained disconnected to implement the worst-case scenario. One of the three-phase SMA Sunny Island inverters was synchronized with the main grid and charged the battery banks. Figure 12 provides an overview of the MG state during the experiment, regarding the load, generation, EV, and the grid. The SMA Sunny Island inverter was disconnected from

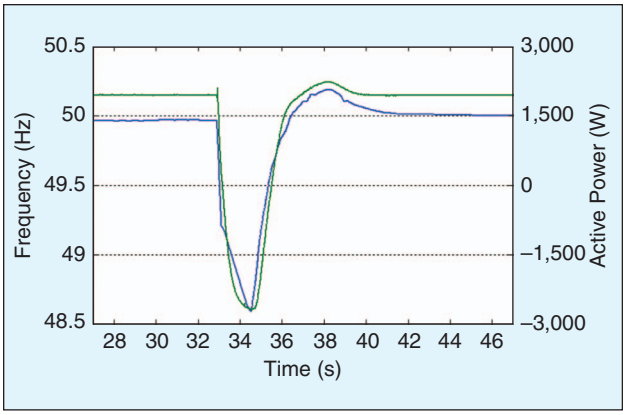

FIGURE 13 The MG frequency (blue) and EV active power (green) during the islanding event.

the main grid at $t = 33$ s to simulate an unplanned islanding event.

Figure 13 compares the MG frequency response and the EV power output after the inverter was disconnected from the main grid. The MG frequency dropped below 48.6 Hz, and because the zero-crossing frequency of the EV droop characteristic dropped below 49.5 Hz, the EV inverted the power flow and began to inject power into the grid. The Sunny Island inverter's secondary control recovered the frequency to 50 Hz in approximately 3 s, and the EV returned to its reference charging power (1.5 kW).

At $t = 100$ s, the microgeneration started to inject power into the grid, and the load began to decrease at $t = 200$ s. When the MG generation exceeded the load, the Sunny Island inverters charged the flooded lead-acid battery bank. After some time, the batteries were full and the frequency began to increase. As shown in Figure 14, for $t = 324$ s, the MG frequency surpassed the EV frequency dead band (50.1 Hz). Thus, the EV increased its charging power to its maximum (3 kW) due to the operation of the frequency droop control. At $t = 500$ s, the

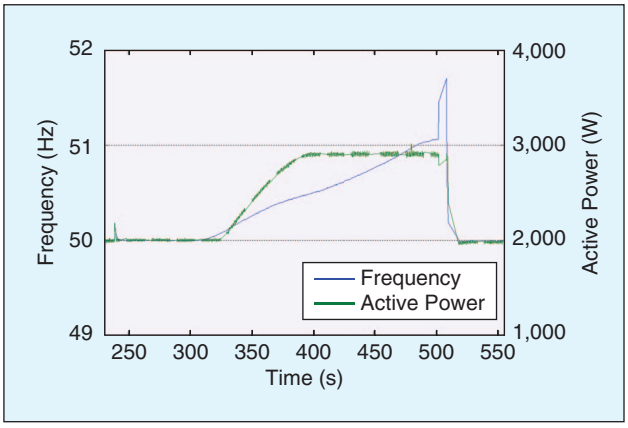

FIGURE 14 The MG frequency response and EV active power output.

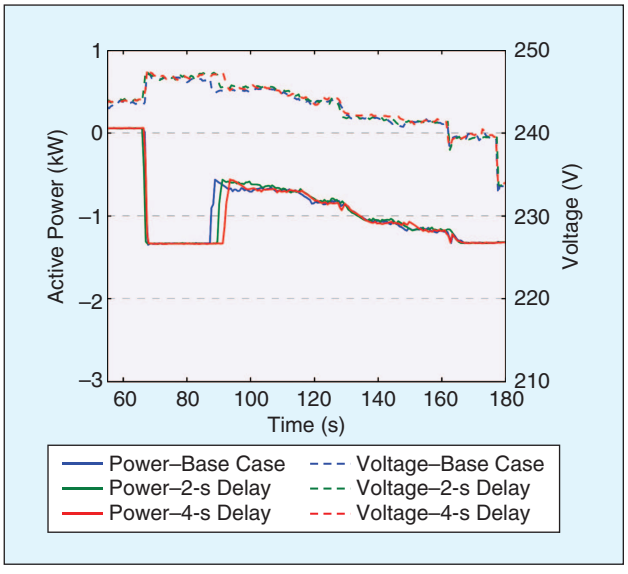

FIGURE 15 The photovoltaic active power and voltage response while considering delays only.

inverters began the resynchronization process, and the MG was reconnected at $t = 510$ s.

Impact of Communications

The MG operation resulted from the combination of the central and local control schemes, and it is important to account for the uncertainty introduced by the communications system to ensure a robust control implementation. Using the medium-behavior controller data exchange, delays and losses were emulated to understand their impact in the MG operation. In a similar experiment, shown in Figure 15 the connection of the photovoltaic inverter to the grid was triggered at $t = 65$ s, followed by the activation of the local droop near $t = 90$ s. Average delays of 2 and 4 s in the communications between the MGCC and local controllers were set in the activation of the droop control. Additional

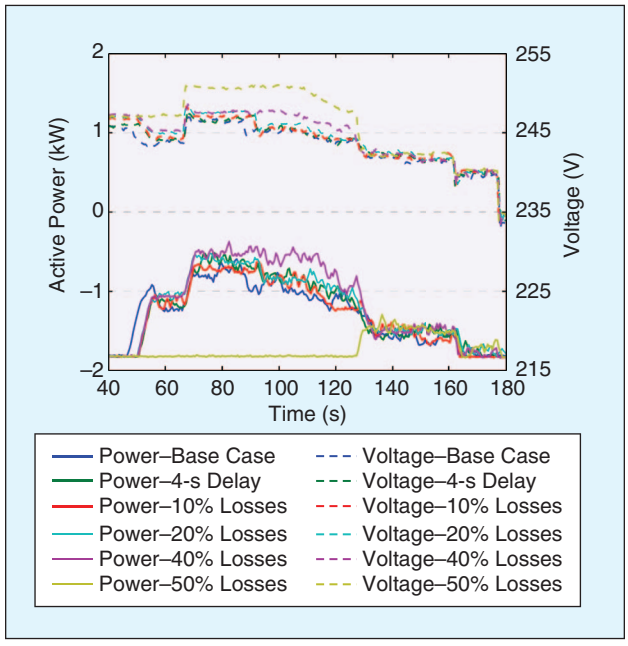

FIGURE 16 The photovoltaic active power and voltage response while considering delays with losses.

experiments were conducted that considered the occurrence of losses in the exchanged data. Figure 16 shows that communication-related failures can have a significant impact in terms of the MG operation.

Conclusions

This integration framework for EVs in electric power systems is capable of dealing with the various system-operation conditions, providing EVs with the capability of being an active element within the grid instead of a typical passive load. In this way, benefits for both system operators and EV owners are expected by granting more resilience and controllability to power systems.

Concerning the methodology presented for a steady state, we have shown that it is appropriate to make expeditious studies in distribution networks. Results have shown that power systems can handle, up to a certain level, the penetration of EVs without considerable changes in the grid if a dumb-charging approach is used. Nevertheless, when the share of EVs reaches a given value, it is necessary to reinforce the grid or implement advanced management and control strategies for EV charging. The results from the experimental tests have shown that the EV management and control methods developed in this article are also effective in real-world environments.

Acknowledgments

This work was supported by the SusCity project (MITPTB/CS/0026/2013) and by the Smart Guide project (SmartGP/0002/2015), both financed by Fundação para a Ciência e Tecnologia.

Author Information

Filipe J. Soares (filipe.j.soares@inesctec.pt) received his B.S. and Ph.D. degrees in sustainable energy systems through the Massachusetts Institute of Technology Portugal Program, both from the University of Porto, Portugal, in 2004 and 2012, respectively. He is currently a senior researcher for the Centre for Power and Energy Systems at the Institute for Systems and Computer Engineering of Porto, Portugal. His research activities are directed toward the integration of renewable energy sources and electric vehicles in distribution grids, energy efficiency, and demand-response functionalities.

David Rua (drua@inesctec.pt) received his B.S. degree in electrical engineering from the Faculty of Engineering of the University of Porto (FEUP), Portugal, in 2006, his M.Sc. degree in electrical engineering from the Instituto Superior Técnico, Lisboa, Portugal, in 2008, and his Ph.D. degree in sustainable energy systems from FEUP, in 2014. He is a researcher at the Institute for Systems and Computer Engineering of Porto, Portugal, and is interested in areas that involve the use of communications systems for electric networks operation and the management of energy resources to provide flexibility services.

Clara Gouveia (clara.s.gouveia@inesctec.pt) received her M.S. degree in electrical engineering from the Faculty of Engineering of the University of Porto, Portugal, in 2008, where she is currently working toward her Ph.D. degree in power systems. She is a member of the research team at the Institute for Systems and Computer Engineering of Porto, Portugal, and her research is focused on the development of the MicroGrid concept, integrating plugged-in electrical vehicles in the operation of the electric system.

Bruna D. Tavares (bruna.c.tavares@inesctec.pt) received her M.S. degree in electrical and computer engineering from the Faculty of Engineering at the University of Porto, Portugal, in 2016. She is a researcher for the Centre for Power and Energy Systems at the Institute for Systems and Computer Engineering of Porto, Portugal. Her research activities are directed toward the integration of distributed energy resources in distribution grids and the development of advanced algorithms and functionalities for their planning and management.

António M. Coelho (antonio.m.coelho@inesctec.pt) received his M.S. degree in electrical and computer engineering from the Faculty of Engineering at the University of Porto, Portugal, in 2015. He is a researcher for the Centre for Power and Energy Systems at the Institute for Systems and Computer Engineering of Porto, Portugal. His research activity is directed toward the integration of distributed energy resources in distribution grids.

João A.P. Lopes (jpl@fe.up.pt) received his B.S. and Ph.D. degrees in electrical engineering from the University of Porto, Portugal, in 1981 and 1988, respectively. Since 2008, he has been a full professor in the Department of Electrical and Computer Engineering, Faculty of Engineering, University of Porto. He is also a director of the Institute for Systems and Computer Engineering of Porto, Portugal. He is a Senior Member of the IEEE.

References

[1] H. Turker, A. Florescu, S. Bacha, and D. Chatroux, "Voltage profile and excess subscription assessments indexes based on random selection of real daily loads profiles (DLPs) on residential electric grid areas for a high penetration of plug-in hybrid electric vehicles (PHEVs)," in *Proc. 2011 IEEE Vehicle Power and Propulsion Conf.*, Chicago, IL, pp. 1–5.

[2] T. K. Lee and Z. S. Filipi, "Response surface modeling approach for the assessment of the PHEV impact on the grid," in *Proc. 2011 IEEE Vehicle Power and Propulsion Conf.*, Chicago, IL, pp. 1–6.

[3] P. Dost, F. Einwachter, P. Spichartz, and C. Sourkounis, "Influence of electric vehicle charging demands on the grid load based on fleet measurements," in *Proc. 2014 IEEE Vehicle Power and Propulsion Conf.*, Coimbra, Portugal, pp. 1–6.

[4] G. Lacey and G. Putrus, "Controlling EV charging schedules: Supporting the grid and protecting battery life," in *Proc. 2015 IEEE Vehicle Power and Propulsion Conf.*, Montréal, QC, Canada, pp. 1–5.

[5] A. Soares, H. Melo, C. H. Antunes, J. P. Trovao, A. Gomes, and H. Jorge, "Integration of the electric vehicle as a manageable load in a residential energy management system," in *Proc. 2015 IEEE Vehicle Power and Propulsion Conf.*, Montréal, QC, Canada, pp. 1–6.

[6] V. Monteiro, J. G. Pinto, and J. L. Afonso, "Operation modes for the electric vehicle in smart grids and smart homes: Present and proposed modes," *IEEE Trans. Veh. Technol.*, vol. 65, no. 3, pp. 1007–1020, Mar. 2016.

[7] R. Torabikalaki and A. Gomes, "Optimizing the coordinated charging of a group of electric vehicles," in *Proc. 2014 IEEE Vehicle Power and Propulsion Conf.*, Coimbra, Portugal, pp. 1–6.

[8] A. Khaligh and Z. Li, "Battery, ultracapacitor, fuel cell, and hybrid energy storage systems for electric, hybrid electric, fuel cell, and plug-in hybrid electric vehicles: State of the art," *IEEE Trans. Veh. Technol.*, vol. 59, no. 6, pp. 2806–2814, July 2010.

[9] N. Hatziargyriou, N. Jenkins, G. Strbac, J. A. Lopes, J. Ruela, A. Engler, J. Oyarzabal, G. Karinotakis, A. Amorim. "Microgrids—Large scale integration of microgeneration to low voltage grids," in *Proc. Conseil International des Grands Réseaux Électriques 2006*.

[10] J. A. Peças Lopes, C. L. Moreira, and A. G. Madureira, "Defining control strategies for microgrids islanded operation," *IEEE Trans. Power Syst.*, vol. 21, no. 2, pp. 916–924, May 2006.

[11] J. Ruela, J. Anduaga, J. Oyarzabal, and S. Macedo. (2005). MicroGrids project deliverable DF1: Report on telecommunication infrastructures and communication protocols. INESC Porto, Portugal, and LABEIN, Spain. [Online]. Available: http://www.microgrids.eu/micro2000/delivarables/Deliverable_DF1.pdf

[12] J. A. Peças Lopes, F. J. Soares, and P. M. Rocha Almeida, "Integration of electric vehicles in the electric power system," *Proc. IEEE*, vol. 99, pp. 168–183, Jan. 2011.

[13] A. G. Madureira, J. C. Pereira, N. J. Gil, J. A. Peças Lopes, G. N. Korres, and N. D. Hatziargyriou. "Advanced control and management functionalities for multi-microgrids," *Eur. Trans. Elect. Power*, vol. 21, no. 2, pp. 1159–1177, Mar. 2011.

[14] I. Guedes. (2000). Inquérito à mobilidade da população residente (in Portuguese). Instituto Nacional de Estatística. Porto, Portugal. [Online]. Available: https://www.google.pt/url?sa=t&rct=j&q=&esrc=s&source=web&cd=2&cad=rja&uact=8&ved=0ahUKEwiivJGFodDYAhWOCuwKHTpIDw4QFggtMAE&url=http%3A%2F%2Fwww.ine.pt%2Fngt_server%2Fattachfileu.jsp%3Flook_parentBoui%3D7415445%26att_display%3Dn%26att_download%3Dy&usg=AOvVaw014Gc9yyRUbIjIkzpbMYru

[15] *Voltage Characteristics of Electricity Supplied by Public Distribution Systems*, EN 50160, 2003.

VT